Dalton Transactions

PAPER

View Article Online
View Journal | View Issue

Cite this: *Dalton Trans.*, 2015, **44**, 15049

The addition of bromine and iodine to palladacyclopentadienyl complexes bearing bidentate heteroditopic P–N spectator ligands derived from differently substituted quinolinic frames. The unexpected evolution of the reaction†

Luciano Canovese,*[a] Fabiano Visentin,[a] Thomas Scattolin,[a] Claudio Santo[a] and Valerio Bertolasi[b]

Received 19th May 2015,
Accepted 19th July 2015

DOI: 10.1039/c5dt01884f

www.rsc.org/dalton

We have synthesized two palladacyclopentadienyl derivatives bearing bidentate ligands heteroditopic 8-(diphenylphosphino)quinoline or 8-(diphenylphosphino)-2-methylquinoline. We have reacted the palladacyclopentadienyl complexes with Br_2 and I_2 to gain clues on the formation mechanism of the corresponding σ-butadienyl derivatives. We were able to obtain the pure σ-butadienyl derivative only in the case of Br_2 reacting with the palladacyclopentadienyl complex bearing the unsubstituted quinoline. However, an equilibrium mixture of the σ-butadienyl and a novel zwitterionic species was obtained when the same complex reacts with I_2. Furthermore, we have obtained exclusively an unprecedented zwitterionic complex when I_2 reacts with the palladacyclopentadienyl complex bearing the substituted quinoline and a different ratio of an equilibrium mixture of σ-butadienyl and the zwitterionic species when the latter derivative reacts with Br_2. The solid state structures of one σ-butadienyl complex and of the two novel zwitterionic derivatives were determined and an interpretation of the observed reactivity based on kinetic data and a computational study has been suggested.

Introduction

A number of catalyzed reactions are based on the stability and chemical versatility of palladium complexes toward oxidative addition and reductive elimination. In particular, interconversion between Pd(0) and Pd(II) derivatives[1] has been widely studied since it often represents the keystone for several cross coupling processes. In contrast, the red–ox reactions involving the Pd(II)–Pd(IV)–Pd(II) conversions are comparatively less investigated and are often related to addition of halogens or organic halides in catalytic[2] or stoichiometric[3] processes yielding conjugated dienes as their final products. The conjugated dienes are important compounds contained in many natural and bioactive products. Therefore, their synthesis is of remarkable importance as testified by the development of catalytic protocols based on cobalt,[4] ruthenium,[5] nickel[6] and palladium.[6b,7] Particular emphasis has been placed on the reactivity of palladacyclopentadienyl derivatives bearing different spectator ligands.[2,3,8] We have recently carried out a detailed study on the oxidative addition of I_2 to palladacyclopentadienyl complexes bearing monodentate isocyanides as spectator ligands. We were able to measure the rates of intramolecular conversion of the intermediate *trans*-diiodo palladium(IV) into the *cis*-diisocyanide-tetramethyl pallada-1-iodobuta-1,3-diene-1,2,3,4-tetracarboxylate, its subsequent isomerisation to the *trans*-isomer, and support the experimental results with a computational study.[9]

We also think that the conversion of the metallacyclopentadienyl complexes into the σ-butadienyl derivatives deserves a further study since the stereospecific formation of the final butadienyl fragment is mainly governed by the transition state and the intermediate structures involved in this first step. We have therefore synthesized two palladacyclopentadienyl complexes bearing the bidentate heteroditopic ligands 8-(diphenyl-

[a]*Dipartimento di Scienze Molecolari e Nanosistemi, Università Ca' Foscari, Venice, Italy. E-mail: cano@unive.it*
[b]*Dipartimento di Chimica e Centro di Strutturistica Diffrattometrica, Università di Ferrara, Ferrara, Italy*

†Electronic supplementary information (ESI) available: Further details of the structure determination, final coordinates, bond distances and bond angles and ORTEP representations for **2a**, **4b** and **5b**, NMR spectra, schematic computational outcomes. CCDC 1053523–1053525. For ESI and crystallographic data in CIF or other electronic format see DOI: 10.1039/c5dt01884f

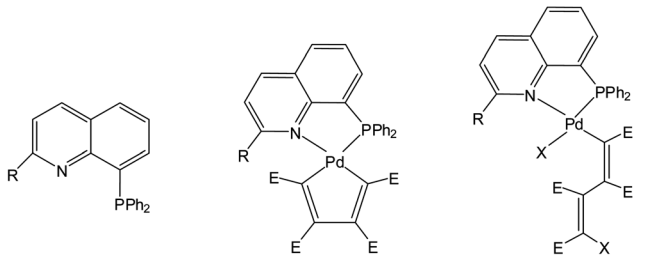

Scheme 1 Ligands, starting complexes and identified σ-butadienyl derivatives.

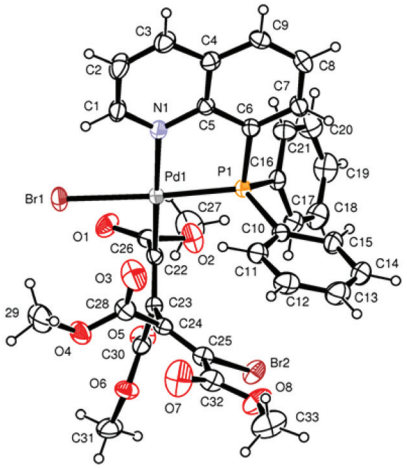

Fig. 1 ORTEP view of complex **2a** showing the thermal ellipsoids at the 30% probability level.

phosphino)quinoline (DPPQ) or 8-(diphenylphosphino)-2-methyl quinoline (DPPQ-Me) which, while avoiding complications arising from *cis–trans* isomerization of the spectator ligands, impart to the palladium derivative properties that could be exploited in insertion reactions,[10] isomerization of a co-ordinated olefin[11] and nucleophilic attack on the allyl fragment.[12] We have finally studied from the experimental and theoretical point of view the oxidative addition of the cited complexes using bromine and iodine.

The ligands, the palladacyclopentadienyl and the identified σ-butadienyl complexes are reported in the following Scheme 1.

Results and discussion

Synthesis of cyclometallated complexes 1a and 1b

The addition in acetone of the ligands DPPQ[13] or DPPQ-Me[14] under an inert atmosphere (Ar) to the polymer $[PdC_4(COOMe)_4]_n$ which was synthesized using published procedures,[15] yields complexes **1a** and **1b** which were easily isolated with good yield. These compounds are characterized by the downfield shift of the phosphorus (*ca.* 40 ppm) and of the quinoline H^2 (complex **1a**) or CH_3 (complex **1b**) protons, with respect to the free ligands in the ^{31}P NMR and ^1H NMR spectra. There are also distinct signals related to four different $COOCH_3$ groups in the ^1H and ^{13}C NMR spectra (see ESI Fig. S1†). Notably, at variance with the pyridylthioether palladacyclopentadienyl species,[8g] complexes **1a** and **1b** display no tendency for rotation of the spectator ligands (*i.e.* exchange of coordination sites between the different donor atoms).

Reactivity of complex 1a with Br_2

As can be seen in Scheme 1, complex **1a** reacts with Br_2 to give the expected σ-butadienyl derivative **2a**. The formation of **2a** is apparent as can be deduced from the ^1H, ^{13}C and ^{31}P NMR spectra in $CDCl_3$ of the reaction product after precipitation from the concentrated reaction mixture with diethyl ether (see ESI Fig. S2†). As a matter of fact, the persistence of four different $COOCH_3$ groups with marked downfield shifts of the quinoline H^2 ($\delta \approx 10.5$ ppm clearly indicating its *cis* position to bromide[12]) compared to those of the precursor, and the phosphorus peak (δ = 34.3 ppm) show the course of the reaction.

Due to its stability in solution and in the solid state it was possible to confirm definitively the structure of **2a** as inferred from NMR, by X-ray diffraction. In Fig. 1 we report the ORTEP[16] representation of the solid state structure of complex **2a** which will be discussed later.

Reactivity of complex 1b with Br_2

The reaction of complex **1b** with bromine under similar experimental conditions gives immediately complex **2b** which can be quantitatively separated from the reaction mixture when precipitation with diethyl ether is induced soon after the addition of the Br_2 and at low temperature (273 K). The NMR spectra of complex **2b** are very similar to those of **2a**. In particular the ^{31}P singlet of the former is almost isochronous to that of the latter (δ = 34.2 ppm) (see ESI Fig. S3†).

Complex **2b**, however, is not stable in solution and in about 30 h undergoes a remarkable change which is evident when the NMR spectra of the starting and the final derivative are compared. In fact, the phosphorus peak shifts upfield by about 20 ppm and the signals ascribable to the four OCH_3 groups resonate in different positions in the ^1H NMR spectrum (see ESI Fig. S4†).

However, the key contribution for understanding the nature of the new species (**4b**) was the determination of its solid state structure which is reported in Fig. 2 (again, the discussion of the structure will be dealt with in another section).

According to the structure of **4b**, the ^{13}C NMR spectrum shows a doublet at *ca.* 42 ppm ($J_{CP} \approx 60$ Hz) and a singlet at *ca.* 31 ppm ascribable to the alkyl carbons bound to the palladium centre.

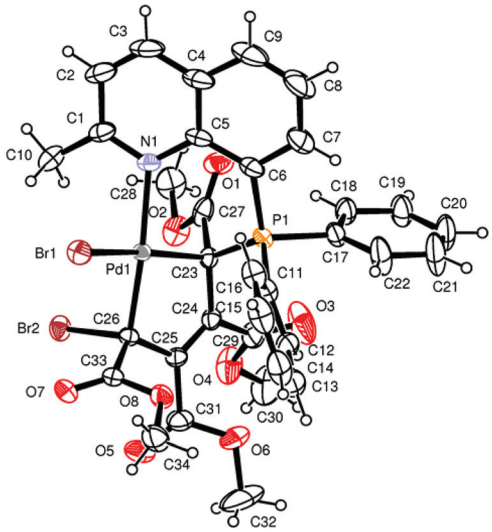

Fig. 2 ORTEP view of complex **4b** showing the thermal ellipsoids at the 30% probability level.

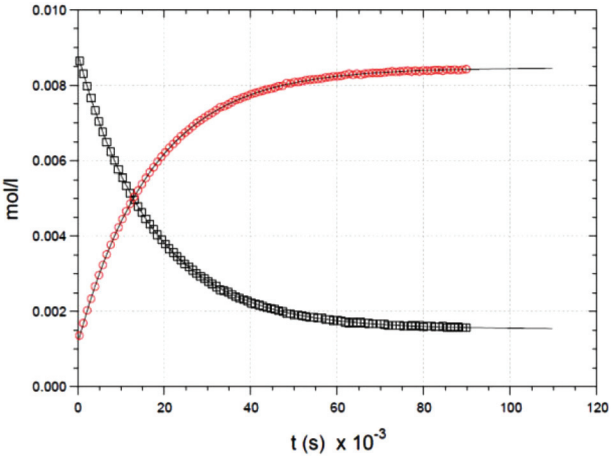

Fig. 3 ^{1}H NMR concentration profiles of **2b** (squares) and **4b** (circles) *vs.* time (s) for the reaction: **2b** = **4b** in $CDCl_3$ at 298 K.

The reaction and the suggested mechanism yielding this unprecedented complex **4b** are shown in eqn (1):

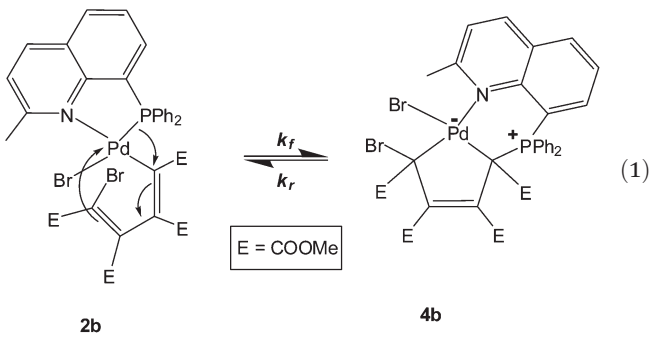

2b 4b (1)

The formation of the zwitterionic complex **4b** might be explained as the result of an intramolecular nucleophilic attack of the phosphorus originally coordinated to the metal on the sp^2 carbon of the butadienyl fragment. The overall process is a slow equilibrium reaction and the amount of complex **2b** that remained unreacted was evaluated to be 15% of its initial concentration ($K_E \approx 5.4$).[17]

Thus, it was possible to calculate k_f and k_r independently by non-linear regression of the concentration *vs.* time data implemented in the SCIENTIST® computing environment (Fig. 3).

The k_f and k_r values were estimated to be $(4.93 \pm 0.01) \times 10^{-5}$ and $(8.93 \pm 0.02) \times 10^{-6}$ s^{-1}, respectively.[18] The equilibrium constant was calculated as $K = k_f/k_r = 5.52 \pm 0.02$ which is in good agreement with the value determined from the experimentally detected final concentrations of species **2b** and **4b** ($K \approx 5.4$) (see also footnote SI 1 in the ESI†).

It is noteworthy that it was not possible to obtain derivative **4a** from complex **1a**. As a matter of fact, when the reaction of complex **1a** with Br_2 was carried out for a prolonged time at high temperature in $CDCl_3$ (323 K) a massive decomposition occurred.

Reactivity of complex 1b with I_2

The addition at RT of an equimolecular amount of I_2 to a solution of **1b** in CH_2Cl_2 gives readily and quantitatively complex **5b** as the only reaction product (eqn (2)).

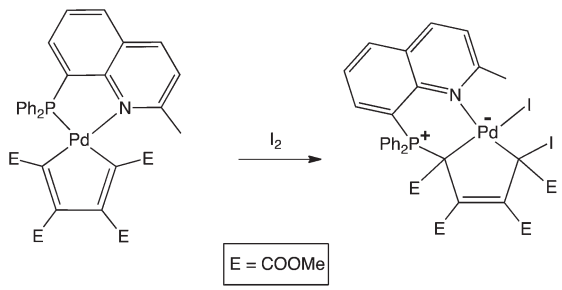

1b 5b (2)

Complex **5b** displays NMR spectra very similar to those of complex **4b** previously described; in particular, the single signal in the ^{31}P NMR spectrum resonates at 8.9 ppm, whereas the ^{13}C NMR spectrum shows the characteristic peaks of the Pd–*C*–PPh_2 (doublet at *ca.* 44 ppm, J_{CP} = 61.8 Hz) and Pd–*C*–I (singlet at 32.9 ppm) (see ESI Fig. S5†). Again the structure of derivative **5b** was definitively resolved by X-ray diffractometry as reported in the Crystal structure determination section (Fig. 4).

However, when the reaction is carried out at a low temperature (253 K) it is possible to observe the formation of complex **3b** which was identified on the basis of the similarity of its ^{1}H and ^{31}P NMR spectra with those of the parent complex **3a** (*vide infra*). As expected, complex **3b** readily reverts to complex **5b** at RT (see ESI Fig. S6†).

Complex **1a** when reacting with I_2 predictably takes the middle course and an equilibrium mixture of the σ-butadienyl **3a** and zwitterionic **5a** complexes is detectable in solution. In Fig. 5 the ^{1}H and ^{31}P NMR spectra of the equilibrium mixture of complexes **3a** and **5a** taken soon after the addition of I_2 to

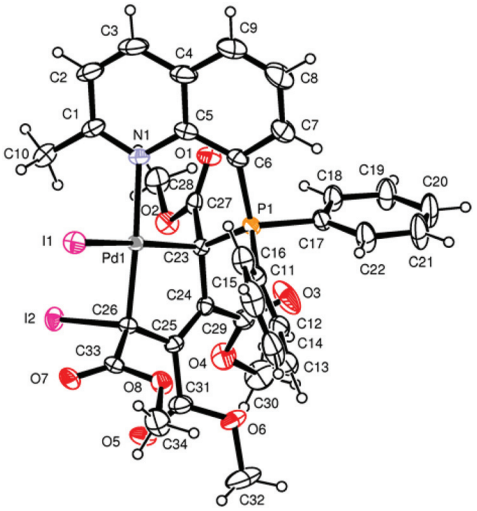

Fig. 4 ORTEP view of complex **5b** showing the thermal ellipsoids at the 30% probability level.

1a are reported. Remarkably, the immediately established concentration ratio between isomers remains constant over time.

A summary of the oxidative additions of Br_2 and I_2 on complexes **1a** and **1b** is reported in the following Scheme 2 in which the complexes within dotted squares (**4a**, **3b**) have not been isolated.

Reactivity of complex 2b with I^-

In order to gain some more information about the driving force promoting the widening of the coordinative ring, we have reacted complex **2b** ($[\mathbf{2b}]_0 \approx 1 \times 10^{-2}$ mol dm^{-3}) with two equivalents of $(n\text{-Bu})_4NI$, in CD_2Cl_2 at 298 K. The ^1H and ^{31}P NMR spectra of the reaction mixture in CD_2Cl_2 show that an equilibrium reaction between the starting complex **2b** and a new species **2b*** is immediately established. Complex **2b*** was formed as a consequence of the substitution of the Br^- coordinated to palladium with iodide. The equilibrium mixture is slowly converted into a new equilibrium mixture of the zwitterions **4b** and **4b***, as summarized in Scheme 3. The presence of complex **4b** was proved by comparison with the ^1H and ^{31}P NMR spectra of an authentic sample of **4b**. The structure of **4b*** was instead assessed by the comparison with the ^1H and ^{31}P NMR spectra of the complex obtained by reacting complex **4b** with an excess (2 : 1) of $(n\text{-Bu})_4NI$ (**6c**). In the latter case, only the bromide coordinated to palladium should be substituted according to the well-established theory of nucleophilic substitution on square planar complexes[19] (see Scheme 3 and ESI Fig. S7a–c†).

As already stated, complex **3b** is not stable and immediately gives zwitterion **5b** at RT. In contrast, since the parent complex **2b*** reacts slowly to yield zwitterion **4b*** it is reasonable to surmise that the halide bound to sp^2 carbon is also a determinant in modulating the reaction rate. In summary, the rate of the reaction yielding the zwitterionic complexes seems to be due to an interplay of three different factors, *i.e.* the distortion of the coordinating ring,[10a,b,11,20] the *trans* influence of the halide *trans* to quinoline phosphorus, and the charge density on the butadienyl sp^2 carbon (which is clearly influenced by the electronegativity of the bound halide). Therefore, the best combination favoring the widening of the coordinated ring is the presence of the methyl substituted quinoline (and the consequent induced distortion of the original coordinative ring), the iodide *trans* to quinoline phosphorus, and the

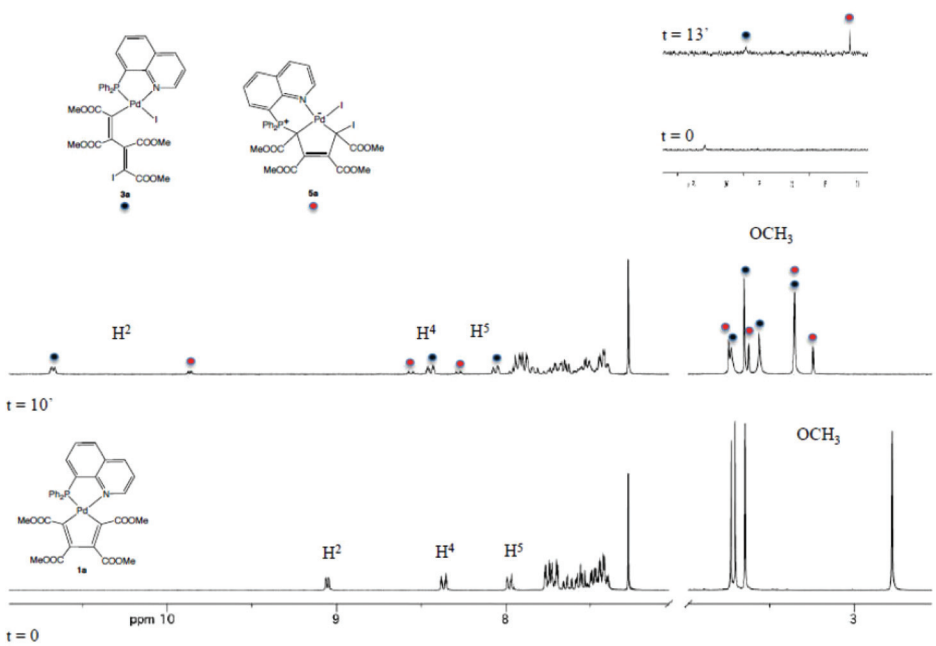

Fig. 5 ^1H and ^{31}P NMR spectra of the starting complex **1a** (bottom) and of the equilibrium mixture of complexes **3a** and **5a** (top) in $CDCl_3$ at 298 K.

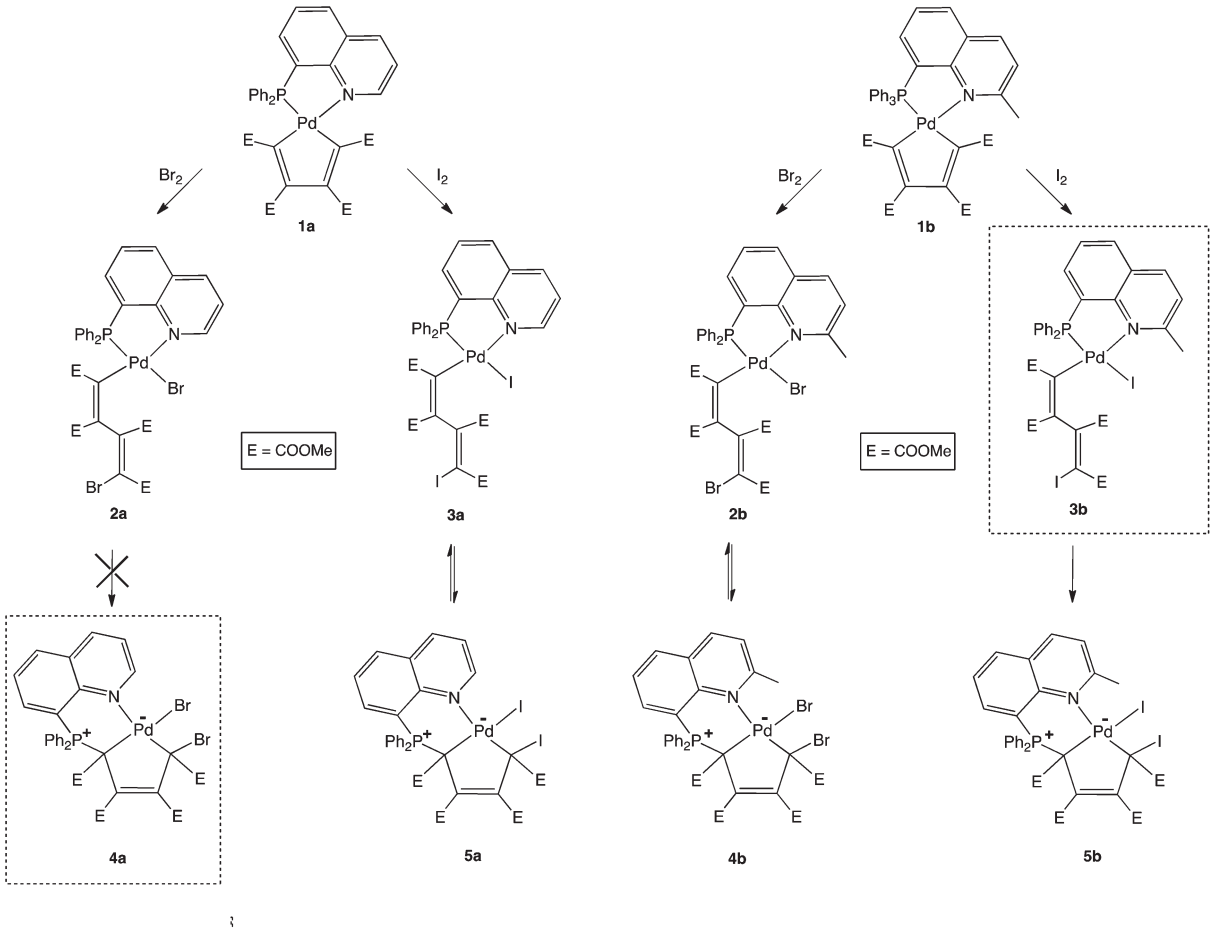

Scheme 2 General overview of the reactivity of complexes **1a** and **1b** towards the addition of Br_2 and I_2 (within the dotted squares the not isolated products).

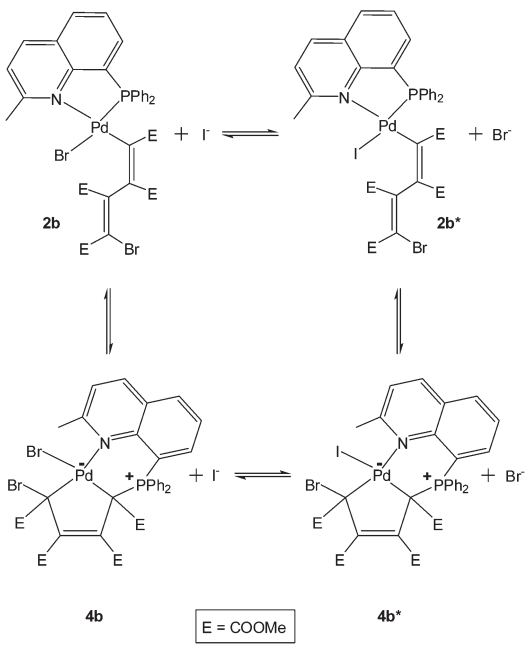

Scheme 3 Schematic representation of the equilibrium reactions triggered by the addition of $(n\text{-Bu})_4NI$ to complex **2b** in CD_2Cl_2 at RT.

iodide bound to the butadienyl sp^2 carbon. Conversely, the other end is represented by the unsubstituted quinoline and the bromides bound to the palladium and to butadienyl sp^2 carbon.

Computational study

Such experimental observations were not in contrast to a detailed computational study carried out by the Gaussian 09 program.[21] To save computing time the carboxymethyl group COOMe was replaced by the less disordered CN moiety (in the following discussion the CN derivatives will maintain the same labels of the original complexes marked with an apex).

Taking into account the limitations due to the errors implicit in this sort of calculation ($\Delta\Delta G^\circ \approx \pm 2$ kcal mol^{-1}) and the replacement of COOMe with CN groups, it was calculated that:

(i) complex **4b′** is more stable than complex **2b′** by 2.3 kcal mol^{-1}.

(ii) complex **5b′** is more stable than complex **3b′** by 5.0 kcal mol^{-1}.

(iii) complex **4a′** is less stable than complex **2a′** by 0.9 kcal mol^{-1}.

(iv) complex **5a′** is less stable than complex **3a′** but the difference is reduced if compared with the former (ΔG° = 0.5 kcal mol^{-1}).

(See ESI Fig. S8† for a schematic comparison).

The assessed energy values agree with the experimental results and in particular they account for the observed equilibrium distribution between complexes **2b′** and **4b′** (ΔG° = 2.3 kcal mol^{-1}) and complexes **3a′** and **5a′** (ΔG° = 0.5 kcal mol^{-1}). The higher difference in energy between complex **3b′** and **5b′** (ΔG° = 5.0 kcal mol^{-1}) is consistent with the fact that complex **5b** was the only isolated species, but it does not fully explain the behavior of complexes **2a′** and **4a′**. Although the higher energy of complex **4a′** is clearly apparent, the calculated $\Delta\Delta G^\circ$ (0.9 kcal mol^{-1}) would be indicative of an equilibrium distribution.

However, since no equilibrium is experimentally observed, we think that this fact might depend on kinetic factors which are modulated by the interplay between the less destabilizing nature of bromide toward phosphorus (the *trans*-influence of bromide being lower than that of iodide) and the higher stability of the undistorted chelating ring of the DPPQ. More simply, it could just be the intrinsic uncertainty typical of this sort of calculations.

Crystal structure determination

An ORTEP[16] view of neutral complex **2a** is shown in Fig. 1. A selection of bond distances and angles is given in Table S2.† The geometry around the Pd centre is a slightly distorted square planar. The four positions around the central Pd are occupied by the carbon C_α of the 1,2,3,4-tetrakis(methoxycarbonyl)buta-1,3-diene-4-Br-1-yl anionic ligand, a Br anion, the pyridine nitrogen and phosphorus of the 8-diphenylphosphanyl-quinoline (DPPQ) ligand. The deviations from the basal plane are: −0.0004(4) for Br1, 0.016(3) for N1, −0.021(1) for P1 and 0.022(3) Å for C22. Pd1 is situated at 0.0662(3) Å above this average plane. The C22 = C23–C24 = C25 buta-1,3-diene moiety displays an anti-clinal conformation with a torsion angle of −117.0(4)°.

An ORTEP[16] view of the neutral isostructural complexes **4b** and **5b** is shown in Fig. 2 and 4.

A selection of bond distances and angles is given in Table S2.† In both complexes, the geometry around the Pd centre is square planar distorted towards a tetrahedral arrangement. The four positions around the central Pd are occupied by halogen atoms, Br in **4b** or I in **5b**. The pyridine nitrogen of the 8-diphenylphosphanyl-2-methyl-quinoline (DPPQ-Me) ligand and the α,δ-carbons of the buta-1,3-diene-4-Br(or I)-1-yl moiety of the ligand are as in the previous complex **2a**. The deviations of the four atoms from the basal plane are: −0.0053(5) for Br1, 0.224(3) for N1, −0.273(3) for C23 and 0.285(3) Å for C26 with the Pd1 atom at 0.0975(3) Å above this average plane, in complex **4b**. For complex **5b** they are: −0.0019(3) for I1, 0.222(3) for N1, −0.333(3) for C23 and 0.289(3) Å for C26 with the Pd1 atom at 0.1228(3) Å above this average plane, in complex **5b**. In both complexes the Pd1–C23–C24–C25–C26 palladacyclopentene rings are approximately planar with maximum deviations from the mean planes of −0.081(4) for C25 and 0.074(3) Å for C26 in complex **4b** and −0.072(3) for C25 and 0.058(3) Å for C26 in complex **5b**.

The different coordination modes of the buta-1,3-diene ligand in complexes **4b** and **5b** with respect to that observed in complex **2a** give rise to variations both in carbon hybridisations and in C–C bond distances.

Conclusions

The oxidative addition of Br_2 or I_2 to palladacyclopentadienyl complexes bearing the bidentate DPPQ or DPPQ-Me as spectator ligands yields different derivatives depending on the nature of the ancillary ligands and halogens. Thus, complex **1a** reacts with Br_2 yielding the σ-butadienyl derivative **2a** and complex **1b** with I_2 to give the unprecedented zwitterionic complex **5b**, only. The cross reactivity yields in both cases an equilibrium mixture of the σ-butadienyl and zwitterionic complexes **2b** and **4b** (in the case of complex **1b** reacting with Br_2) and **3a** and **5a** (in the case of complex **1a** reacting with I_2). The experimental results and in particular the reactivity of the butadienyl derivatives were interpreted taking into account the different lability of the bidentate ligands (DPPQ-Me which is more labile than DPPQ), the higher *trans*-influence of I^- compared to Br^-, and the charge density on the butadienyl sp^2 carbon which is modulated by the electronegativity of the bound halide. In order to give adequate support to the experimental observations a detailed study of the solid state structure of complexes **2a**, **4b** and **5b** together with the determination of the reaction rates characterizing the equilibrium reaction between **2b** and **4b** were also carried out.

Experimental

Solvents and reagents

All the following distillation processes were carried out under an inert atmosphere (argon). Acetone and CH_2Cl_2 were distilled over 4 Å molecular sieves and CaH_2 respectively. All the other chemicals were commercially available grade products and were used as purchased.

Data analysis. Nonlinear analysis of the data related to equilibrium and kinetics measurements was performed by locally adapted routines written in the SCIENTIST® environment.

IR and NMR measurements

The IR, ^{1}H, ^{13}C and ^{31}P NMR spectra were recorded on a Perkin-Elmer Spectrum One spectrophotometer and on a Bruker 300 Avance spectrometer, respectively.

Computational details

The geometrical optimization of the complexes was carried out without symmetry constraints, using the hyper-GGA functional M06[22,23] in combination with polarized triple-ζ-quality basis

sets (LAN2TZ(f))[24,25] and relativistic pseudopotential for the Pd atoms, a polarized double-ζ-quality basis set (LANL2DZdp)[26] with diffuse functions for the halogen atoms and a polarized double-ζ-quality basis set (6-31G(d,p)) for the other elements.

Solvent effects (dichloromethane, ε = 8.93) were included using CPCM.[27,28]

The "restricted" formalism was applied in all the calculations. By means of the stationary points characterized by IR simulation, the zero-point vibrational energies and thermodynamic parameters were obtained.[29]

The software used was Gaussian 09[21] and all the computational work was carried out on Intel based × 86 − 64 workstations.

Crystal structure determinations

The crystal data of compounds **2a**, **4b** and **5b** were collected at room temperature using a Nonius Kappa CCD diffractometer with graphite monochromated Mo-Kα radiation. The data sets were integrated with the Denzo-SMN package[30] and corrected for Lorentz, polarization and absorption effects (SORTAV).[31] The structures were solved by direct methods using the SIR97[32] system of programs and refined using full-matrix least-squares with all non-hydrogen atoms anisotropically and hydrogens included on calculated positions, riding on their carrier atoms.

All calculations were performed using SHELXL-97[33] and PARST[34] implemented in the WINGX[35] system of programs. The crystal data are given in Table S3.†

Crystallographic data have been deposited at the Cambridge Crystallographic Data Centre and allocated the deposition numbers CCDC 1053523, 1053524, and 1053525.

Synthesis of the ligands and starting complex

The ligands DPPQ,[12] DPPQ-Me[13] and the polymeric complex $[PdC_4(COOMe)_4]_n$[15] were synthesized according to the published procedures.

Synthesis of complex 1a

In a two necked 100 ml flask 198.0 mg (0.51 mmol) of $[PdC_4(COOMe)_4]_n$ and 172.2 mg (0.55 mmol) of DPPQ were dissolved in 20 ml of anhydrous acetone under an inert atmosphere (Ar). The resulting solution was stirred for 1 h and concentrated under vacuum to a reduced volume (2–3 ml). Dropwise addition of diethyl ether (5–10 ml) causes the precipitation of the 309.2 mg (87% yield) of the title complex as a yellow-orange microcrystalline product which was filtered off on a gooch filter, carefully washed with diethyl ether and *n*-pentane and dried under vacuum.

^{1}H-NMR (300 MHz, $CDCl_3$, T = 298 K, ppm) δ: 2.77 (s, 3H, OCH_3), 3.64 (s, 3H, OCH_3), 3.71 (s, 3H, OCH_3), 3.73 (s, 3H, OCH_3), 7.39–7.61 (m, 8H, H^3, Ph), 7.64 (ddd, 1H, J = 7.7, 7.2, 1.2 Hz, H^6), 7.66–7.77 (m, 4H, H^5, Ph), 7.98 (d, 1H, J = 7.9 Hz, H^7), 8.37 (dt, 1H, J = 8.5, 1.4 Hz, H^4), 9.06 (dd, 1H, J = 5.0, 1.4 Hz, H^2).

^{31}P{^{1}H}-NMR ($CDCl_3$, T = 298 K, ppm) δ: 33.4.

^{13}C{^{1}H}-NMR ($CDCl_3$, T = 298 K, ppm) δ: 50.5 (CH_3, OCH_3), 50.9 (CH_3, OCH_3), 51.2 (CH_3, OCH_3), 51.3 (CH_3, OCH_3), 122.6 (CH, C^3), 127.8 (d, CH, J_{CP} = 5.5 Hz, C^6), 129.3 (d, C, J_{CP} = 7.8 Hz, C^{10}), 131.1 (CH, C^5), 135.9 (d, C, J_{CP} = 41.7 Hz, C^8), 136.1 (CH, C^7), 139.0 (CH, C^4), 143.2 (C, C═C), 150.1 (C, C═C), 150.9 (d, C, J_{CP} = 21.6 Hz, C^9), 154.9 (CH, C^2), 157.2 (d, C, J_{CP} = 7.5 Hz, C═C), 164.1 (C, C═O), 165.3 (C, C═O), 173.1 (d, C, J_{CP} = 8.0 Hz, C═O), 175.4 (d, C, J_{CP} = 7.4 Hz, C═O), 176.7 (C, C═C).

Anal. calcd for $C_{33}H_{28}NO_8PPd$: C 56.30, H 4.01, N 1.99. Found: C 56.41, H 4.18, N 1.87.

Synthesis of complex 1b

Complex **1b** was obtained following the same procedure as for complex **1a**.

A yellow-orange microcrystalline solid was obtained with a 74% yield.

^{1}H-NMR (300 MHz, $CDCl_3$, T = 298 K, ppm) δ: 2.86 (s, 3H, OCH_3), 2.89 (s, 3H, OCH_3), 3.39 (s, 3H, quinoline–CH_3), 3.68 (s, 3H, CH_3), 3.64 (s, 3H, OCH_3), 7.89 (d, 1H, H^3, J = 9.0 Hz), 8.18 (d, 1H, H^4, J = 9 Hz); 7.42 (m, 10H).

^{31}P{^{1}H}-NMR ($CDCl_3$, T = 298 K, ppm) δ: 30.16.

Anal. calcd for $C_{34}H_{30}NO_8PPd$: C 56.88, H 4.21, N 1.95. Found: C 56.94, H 4.07, N 1.89.

Synthesis of complex 2a

In a two necked 50 ml flask, 71.1 mg (0.10 mmol) of compound **1** dissolved in 10 ml of anhydrous CH_2Cl_2 17.8 mg (0.111 mmol) of Br_2 dissolved in 5 ml of CH_2Cl_2 was added under an inert atmosphere (Ar). The reaction mixture immediately decolorized and after 5 min stirring the solution was evaporated under vacuum to 3–4 ml. The dropwise addition of diethyl ether induces the precipitation of the title complex as a yellow microcrystalline solid. The solid was filtered off on a gooch filter, washed several times with diethyl ether and *n*-pentane and dried under vacuum to obtain 81.7 mg (94% yield) of the complex.

^{1}H-NMR (300 MHz, $CDCl_3$, T = 298 K, ppm) δ: 3.41 (s, 3H, OCH_3), 3.63 (s, 3H, OCH_3), 3.72 (s, 3H, OCH_3), 3.74 (s, 3H, OCH_3), 7.37–7.54 (m, 6H, Ph), 7.65–7.70 (m, 2H, H^3, H^6), 7.82–7.98 (m, 4H, H^7, Ph), 8.05 (d, 1H, J = 8.0 Hz, H^5), 8.43 (dt, 1H, J = 8.3, 1.5 Hz, H^4), 10.47 (dd, 1H, J = 5.1, 1.5 Hz, H^2).

^{31}P{^{1}H}-NMR ($CDCl_3$, T = 298 K, ppm) δ: 34.3.

^{13}C{^{1}H}-NMR ($CDCl_3$, T = 298 K, ppm) δ: 51.3 (CH_3, OCH_3), 52.0 (CH_3, OCH_3), 53.2 (CH_3, OCH_3), 53.3 (CH_3, OCH_3), 120.9 (C, C═CBr), 123.4 (CH, C^3), 127.9 (d, CH, J_{CP} = 6.9 Hz, C^6), 129.6 (d, C, J_{CP} = 9.4 Hz, C^{10}), 130.4 (C, C═C), 131.8 (CH, C^5), 134.4 (d, C, J_{CP} = 44.3 Hz, C^8), 137.0 (CH, C^7), 139.0 (CH, C^4), 142.7 (C, C═C), 150.2 (d, C, J_{CP} = 20.2 Hz, C^9), 156.4 (CH, C^2), 161.8 (C, C═O), 162.5 (C, C═C), 162.9 (C, C═O), 166.3 (C, C═O), 171.4 (d, C, J_{CP} = 2.6 Hz, C═O).

IR (KBr pellets): $\nu_{C=O}$ 1709 cm^{-1}.

Anal. calcd for $C_{33}H_{28}Br_2NO_8PPd$: C 45.89, H 3.27, N 1.62. Found: C 45.73, H 3.18, N 1.54.

Synthesis of complex 2b

Complex **3a** was obtained following similar conditions to complex **2a** but the synthesis was carried out at a low temperature (273 K) and the complex was collected within 10 min.

A pale-yellow microcrystalline solid was obtained with a 61% yield.

^{1}H-NMR (300 MHz, $CDCl_3$, T = 298 K, ppm) δ: 3.32 (s, 3H, quinoline–CH_3), 3.45 (s, 3H, OCH_3), 3.60 (s, 3H, OCH_3), 3.87 (s, 3H, OCH_3), 3.88 (s, 3H, OCH_3), 7.34–7.62 (m, 9H, PPh_2, H^3), 7.76–8.04 (m, 5H, H^5, H^6, H^7, PPh_2), 8.14 (dd, 1H, J = 8.5, 1.6 Hz, H^4).

$^{31}P\{^1H\}$-NMR ($CDCl_3$, T = 298 K, ppm) δ: 34.3.

IR (KBr pellets): $\nu_{C=O}$ 1732, 1716 and 1704 cm^{-1}.

Anal. calcd for $C_{33}H_{28}I_2NO_8PPd$: C 41.38, H 2.95, N 1.46. Found: C 41.21, H 2.97, N 1.32.

Synthesis of complex 4b

Complex **4b** was obtained by reacting complex **1b** and Br_2 under the same experimental conditions described above in the case of complex **2a**. The reaction mixture was stirred for 28 h and the reaction product precipitated by addition of diethyl ether.

A yellow microcrystalline solid was obtained with a 78% yield.

^{1}H-NMR (300 MHz, $CDCl_3$, T = 298 K, ppm) δ: 3.31 (s, 3H, OCH_3), 3.42 (s, 3H, OCH_3), 3.54 (s, 3H, quinoline–CH_3), 3.64 (s, 3H, OCH_3), 3.71 (s, 3H, OCH_3), 7.39–7.62 (m, 9H, PPh_2, H^3, H^7), 7.67–7.81 (m, 3H, H^6, PPh_2), 7.95–8.08 (m, 2H, H^5, PPh_2), 8.28 (dd, 1H, J = 8.5, 1.9 Hz, H^4).

$^{31}P\{^1H\}$-NMR ($CDCl_3$, T = 298 K, ppm) δ: 10.7.

$^{13}C\{^1H\}$-NMR ($CDCl_3$, T = 298 K, ppm) δ: 30.8 (CH_3, quinoline–CH_3), 31.2 (C, Pd–C–Br), 41.7 (d, C, J_{CP} = 59.9 Hz, C–PPh_3), 51.9 (CH_3, OCH_3), 52.0 (CH_3, OCH_3), 52.1 (CH_3, OCH_3), 52.4 (CH_3, OCH_3), 124.9 (CH, C^3), 127.4 (d, C, J_{CP} = 7.0 Hz, C^{10}), 130.5 (d, C, J_{CP} = 65.9 Hz, C^8), 132.4 (CH, C^6), 133.9 (CH, C^5), 137.7 (C, C═C), 138.6 (CH, C^4), 140.4 (d, CH, J_{CP} = 11.4 Hz, C^7), 148.3 (d, C, J_{CP} = 3.0 Hz, C^9), 157.9 (d, C, J_{CP} = 11.5 Hz, C═C), 157.9 (C, C═O), 164.4 (CH, C^2), 166.5 (C, C═O), 170.3 (d, C, J_{CP} = 7.9 Hz, C═O), 171.4 (C, C═O).

IR (KBr pellets): $\nu_{C=O}$ 1722 cm^{-1}.

Anal. calcd for $C_{34}H_{30}Br_2NO_8PPd{\cdot}CH_2Cl_2$: C 43.66, H 3.35, N 1.45. Found: C 43.51, H 3.23, N 1.32.

Synthesis of complex 5b

Complex **5b** was obtained by reacting complex **1b** and I_2 under the same experimental conditions as described above. The reaction mixture was stirred for 10 min and the reaction product precipitated by addition of diethyl ether.

A pale-yellow microcrystalline solid was obtained in 93% yield.

^{1}H-NMR (300 MHz, $CDCl_3$, T = 298 K, ppm) δ: 3.24 (s, 3H, OCH_3), 3.43 (s, 3H, OCH_3), 3.61 (s, 3H, quinoline–CH_3), 3.63 (s, 3H, OCH_3), 3.74 (s, 3H, OCH_3), 7.39–7.80 (m, 12H, PPh_2, H^3, H^7, H^6, PPh_2), 7.98–8.05 (m, 2H, PPh_2), 8.15 (dt, 1H, J = 7.1, 2.3 Hz, H^5), 8.34 (dd, 1H, J = 8.5, 1.9 Hz, H^4).

$^{31}P\{^1H\}$-NMR ($CDCl_3$, T = 298 K, ppm) δ: 8.9.

$^{13}C\{^1H\}$-NMR ($CDCl_3$, T = 298 K, ppm) δ: 32.9 (C, Pd–C–I), 33.6 (CH_3, quinoline–CH_3), 43.8 (d, C, J_{CP} = 61.8 Hz, C–PPh_3), 52.1 (CH_3, OCH_3), 52.2 (CH_3, OCH_3), 52.3 (CH_3, OCH_3), 52.4 (CH_3, OCH_3), 124.7 (CH, C^3), 127.9 (d, C, J_{CP} = 7.0 Hz, C^{10}), 131.3 (d, C, J_{CP} = 66.8 Hz, C^8), 132.4 (CH, C^6), 134.2 (CH, C^5), 135.5 (C, C═C), 139.2 (CH, C^4), 140.8 (d, CH, J_{CP} = 11.0 Hz, C^7), 148.9 (d, C, J_{CP} = 3.0 Hz, C^9), 161.4 (d, C, J_{CP} = 10.5 Hz, C═C), 164.4 (CH, C^2), 165.0 (C, C═O), 166.2 (C, C═O), 169.5 (d, C, J_{CP} = 7.2 Hz, C═O), 171.6 (C, C═O).

IR (KBr pellets): $\nu_{C=O}$ 1718 cm^{-1}.

Anal. calcd for $C_{34}H_{30}I_2NO_8PPd{\cdot}CH_2Cl_2$: C 39.78, H 3.05, N 1.33. Found: C 39.651, H 2.97, N 1.19.

Notes and references

1 (*a*) J. Tsuji, in *Palladium Reagents and Catalysts: Innovations in Organic Synthesis*, Wiley and Sons, New York, 1995, ch. 4; (*b*) L. S. Hegedus, *Coord. Chem. Rev.*, 1996, **147**, 443–545; (*c*) L. S. Hegedus, *Coord. Chem. Rev.*, 1997, **161**, 129–255; (*d*) I. P. Beletskaya and A. V. Cheprakov, *Chem. Rev.*, 2000, **100**, 3009–3066; (*e*) C. Amatore and A. Jutand, *Acc. Chem. Res.*, 2000, **33**, 314–321; (*f*) R. Zimmer, C. U. Dinesh, E. Nandanan and F. A. Khan, *Chem. Rev.*, 2000, **100**, 3067–3125; (*g*) J. A. Marshall, *Chem. Rev.*, 2000, **100**, 3163–3186; (*h*) E.-I. Negishi, in *Handbook of Organopalladium Chemistry for Organic Synthesis*, ed. E.-I. Negishi and A. de Meijere, Wiley-Interscience, New York, 2002, ch. I.1, I.2; (*i*) K. Tamao, T. Hiyama and E.-I. Niegishi, in *30 Years of the Cross-coupling Reaction*, Special issue, *J. Organomet. Chem.*, 2002, **653**, 1–303. (*j*) L. A. Agrofoglio, I. Gillaizeau and Y. Saito, *Chem. Rev.*, 2003, **103**, 1875–1916; (*k*) E. Negishi and L. Anastasia, *Chem. Rev.*, 2003, **103**, 1979–2017; (*l*) G. Zeni and R. C. Larock, *Chem. Rev.*, 2004, **104**, 2285–2309; (*m*) K. C. Nicolaou, P. G. Bulger and D. Sarlah, *Angew. Chem., Int. Ed.*, 2005, **44**, 4442–4489; (*n*) E.-I. Negishi, *Bull. Chem. Soc. Jpn.*, 2007, **80**, 233–257; (*o*) C. J. Elsevier and M. R. Eberhard, in *Comprehensive Organometallic Chemistry III From Fundamentals to Applications*, ed. A. Canty, ed. in Chief, R. H. C. D. Michael and P. Mingos, Elsevier, Amsterdam, Boston, 2007, vol. 8, ch. 8.05, pp. 270–298; (*p*) M. García-Melchor, X. Solans-Monfort and G. Ujaque, in *CC Bond Formation Comprehensive Inorganic Chemistry II (Second Edition): From Elements to Applications, 9*, ed. J. Reedijk and K. R. Poeppelmeier, Elsevier, Amsterdam, 2013, pp. 767–805.

2 (*a*) M. W. Van Laren and C. J. Elsevier, *Angew. Chem., Int. Ed.*, 1999, **38**, 3715–3717; (*b*) K. Muñiz, *Angew. Chem., Int. Ed.*, 2009, **48**, 2–14; (*c*) L.-M. Xu, B.-J. Li, Z. Yang and Z.-J. Shi, *Chem. Soc. Rev.*, 2010, **39**, 712–733; (*d*) Y. Dang, S. Qu, J. W. Nelson, H. D. Pham, Z.-X. Wang and X. Wang, *J. Am. Chem. Soc.*, 2015, **137**, 2006–2014.

3 (*a*) R. Van Belzen, R. A. Klein, H. Kooijman, N. Veldman, A. L. Spek and C. J. Elsevier, *Organometallics*, 1998, **17**, 1812–1825; (*b*) R. Van Belzen, C. J. Elsevier, A. Dedieu,

N. Veldman and A. L. Spek, *Organometallics*, 2003, **22**, 722–736; (*c*) A. R. Dick, J. W. Kampf and M. S. Sanford, *J. Am. Chem. Soc.*, 2005, **127**, 12790–12791; (*d*) J. Vicente, A. Arcas, F. Juliá Hernández and D. Bautista, *Angew. Chem., Int. Ed.*, 2011, **30**, 6896–6899.

4 (*a*) Y. Wakatsuki, K. Aoki and H. Yamazaki, *J. Am. Chem. Soc.*, 1979, **101**, 1123–1130; (*b*) J. M. O'Connor, M.-C. Chen, M. Frohn, A. L. Rheingold and I. A. Guzei, *Organometallics*, 1997, **16**, 5589–5591; (*c*) E. Shirakawa, Y. Imazaki and T. Hayashi, *Chem. Lett.*, 2008, **37**, 654–655.

5 (*a*) B. M. Trost, A. F. Indolese, T. J. J. Muller and B. Treptow, *J. Am. Chem. Soc.*, 1995, **117**, 615–623; (*b*) J. Le Paih, S. Dérien, I. Ozdemir and P. H. Dixneuf, *J. Am. Chem. Soc.*, 2000, **122**, 7400–7401; (*c*) R. Morita, E. Shirakawa, T. Tsuchimoto and Y. Kawakami, *Org. Biomol. Chem.*, 2005, **3**, 1263–1268.

6 (*a*) E.-I. Negishi, T. Takahashi, S. Baba, D. E. Van Horn and N. Okukado, *J. Am. Chem. Soc.*, 1987, **109**, 2393–2401; (*b*) E. Shirakawa, G. Takahashi, T. Tsuchimoto and Y. Kawakami, *Chem. Commun.*, 2001, 2688–2689.

7 (*a*) F. Tellier, R. Sauvêtre and J. F. Normant, *J. Organomet. Chem.*, 1986, **303**, 309–315; (*b*) J. K. Stille and B. L. Groh, *J. Am. Chem. Soc.*, 1987, **109**, 2393–2401; (*c*) J.-H. Li, Y. Liang and Y.-X. Xie, *J. Org. Chem.*, 2004, **69**, 8125–8127; (*d*) H. Hattori, M. Katsukawa and Y. Kobayashi, *Tetrahedron Lett.*, 2005, **46**, 5871–5875.

8 (*a*) K. Moseley and P. M. Maitlis, *J. Chem. Soc. D*, 1971, 1604–1605; (*b*) H. Suzuki, K. Itoh, Y. Ishii, K. Simon and J. A. Ibers, *J. Am. Chem. Soc.*, 1976, **98**, 8494–8500; (*c*) R. Van Belzen, H. Hoffmann and C. J. Elsevier, *Angew. Chem., Int. Ed. Engl.*, 1997, **36**, 1743–1745; (*d*) E. Shirakawa, H. Yoshida, Y. Nakao and T. Hiyama, *J. Am. Chem. Soc.*, 1999, **121**, 4290–4291; (*e*) Y. Yamamoto, T. Ohno and K. Itoh, *Chem. Commun.*, 1999, 1543–1544; (*f*) H. Yoshida, E. Shirakawa, Y. Nakao, Y. Honda and T. Hiyama, *Bull. Chem. Soc. Jpn.*, 2001, **74**, 637–647; (*g*) L. Canovese, F. Visentin, G. Chessa, P. Uguagliati, C. Levi and A. Dolmella, *Organometallics*, 2005, **24**, 5537–5548.

9 L. Canovese, F. Visentin and C. Santo, *J. Organomet. Chem.*, 2014, **770**, 6–13.

10 (*a*) L. Canovese, F. Visentin, C. Santo, C. Levi and A. Dolmella, *Organometallics*, 2007, **26**, 5590–5601; (*b*) L. Canovese, F. Visentin, C. Santo and V. Bertolasi, *Organometallics*, 2014, **33**, 1700–1709.

11 L. Canovese, F. Visentin and C. Santo, *Organometallics*, 2008, **27**, 3577–3581.

12 L. Canovese, F. Visentin, C. Santo, G. Chessa and V. Bertolasi, *Organometallics*, 2010, **29**, 3027–3038.

13 P. Whehman, H. M. A. van Donge, A. Hagos, P. C. J. Kamer and P. V. N. M. van Leeuwen, *J. Organomet. Chem.*, 1997, **535**, 183–193.

14 L. Canovese, F. Visentin, G. Chessa, C. Santo, P. Uguagliati and G. Bandoli, *J. Organomet. Chem.*, 2002, **650**, 43–56.

15 K. Moseley and P. M. Maitlis, *J. Chem. Soc., Dalton Trans.*, 1974, 169–175.

16 M. N. Burnett and C. K. Johnson, ORTEP III, Report ORNL-6895, Oak Ridge National Laboratory, Oak Ridge, TN, 1996.

17 Thanks to the reduced solubility of zwitterionic complex **4b** in CH_2Cl_2 compared to that of complex **2b**, it was possible to separate crystals for diffractometric determination from the equilibrium mixture. In contrast, any attempts at separating suitable crystals of complex **2b** were unsuccessful since only some crystals of complex **4b** were obtained after about a week at 263 K.

18 As can be seen in Fig. 3 the starting concentration ($t = 0$) of complex **4b** is not null (the estimated values ensuing from the regression analysis are $[\mathbf{2b}] = 8.8 \times 10^{-3} \pm 4 \times 10^{-6}$, $[\mathbf{4b}] = 1.16 \times 10^{-3} \pm 4 \times 10^{-6}$). Since the reaction was carried out starting from an authentic sample of **2b** which was isolated pure some days before the NMR study, we think that the interconversion reaction is also likely to occur in the solid state.

19 M. L. Tobe, in *Inorganic Reaction Mechanisms Nelson Ed*, London, 1972.

20 (*a*) L. Canovese, F. Visentin, G. Chessa, P. Uguagliati, C. Santo and A. Dolmella, *Organometallics*, 2005, **24**, 3297–3308; (*b*) L. Canovese, F. Visentin, G. Chessa, C. Santo and A. Dolmella, *Dalton Trans.*, 2009, 9475–9485.

21 M. J. Frisch, G. W. Trucks, H. B. Schlegel, G. E. Scuseria, M. A. Robb, J. R. Cheeseman, G. Scalmani, V. Barone, B. Mennucci, G. A. Petersson, H. Nakatsuji, M. Caricato, X. Li, H. P. Hratchian, A. F. Izmaylov, J. Bloino, G. Zheng, J. L. Sonnenberg, M. Hada, M. Ehara, K. Toyota, R. Fukuda, J. Hasegawa, M. Ishida, T. Nakajima, Y. Honda, O. Kitao, H. Nakai, T. Vreven, J. A. Montgomery Jr., J. E. Peralta, F. Ogliaro, M. Bearpark, J. J. Heyd, E. Brothers, K. N. Kudin, V. N. Staroverov, R. Kobayashi, J. Normand, K. Raghavachari, A. Rendell, J. C. Burant, S. S. Iyengar, J. Tomasi, M. Cossi, N. Rega, J. M. Millam, M. Klene, J. E. Knox, J. B. Cross, V. Bakken, C. Adamo, J. Jaramillo, R. Gomperts, R. E. Stratmann, O. Yazyev, A. J. Austin, R. Cammi, C. Pomelli, J. W. Ochterski, R. L. Martin, K. Morokuma, V. G. Zakrzewski, G. A. Voth, P. Salvador, J. J. Dannenberg, S. Dapprich, A. D. Daniels, Ö. Farkas, J. B. Foresman, J. V. Ortiz, J. Cioslowski and D. J. Fox, *Gaussian 09, Revision D.01, Gaussian 09*, Gaussian, Inc., Wallingford, CT, 2009.

22 Y. Zhao and D. G. Truhlar, *Acc. Chem. Res.*, 2008, **41**, 157–167.

23 Y. Zhao and D. G. Truhlar, *Theor. Chem. Acc.*, 2008, **120**, 215–241.

24 P. J. Hay and W. R. Wadt, *J. Chem. Phys.*, 1985, **82**, 270–283, 299–310.

25 L. E. Roy, P. J. Hay and R. L. Martin, *J. Chem. Theory Comput.*, 2008, **4**, 1029–1031.

26 C. E. Check, T. O. Faust, J. M. Bailey, B. J. Wright, T. M. Gilbert and L. S. Sunderlin, *J. Phys. Chem. A*, 2001, **105**, 8111–8116.

27 V. Barone, M. Cossi and J. Tomasi, *J. Chem. Phys.*, 1997, **107**, 3210–3221.

28 V. Barone and M. Cossi, *J. Phys. Chem. A*, 1998, **102**, 1995–2001.
29 (*a*) C. J. Cramer, *in Essentials of Computational Chemistry*, John Wiley and Sons, Chichester, 2nd edn, 2004; (*b*) F. Jensen, *in Introduction to Computational Chemistry*, John Wiley and Sons, Chichester, 2nd edn, 2007.
30 Z. Otwinowski and W. Minor, in *Methods in Enzymology, Part A*, ed. C. W. Carter and R. M. Sweet, Academic Press, London, 1997, vol. 276, pp. 307–326.
31 R. H. Blessing, *Acta Crystallogr., Sect. A: Fundam. Crystallogr.*, 1995, **51**, 33–38.
32 A. Altomare, M. C. Burla, M. Camalli, G. L. Cascarano, C. Giacovazzo, A. Guagliardi, A. G. Moliterni, G. Polidori and R. Spagna, *J. Appl. Crystallogr.*, 1999, **32**, 115–119.
33 G. M. Sheldrick, *SHELX-97, Program for Crystal Structure Refinement*, University of Gottingen, Germany, 1997.
34 M. Nardelli, *J. Appl. Crystallogr.*, 1995, **28**, 659–660.
35 L. J. Farrugia, *J. Appl. Crystallogr.*, 1999, **32**, 837–838.